Journal of Heat and Mass Transfer Research

Journal homepage: http://jhmtr.journals.semnan.ac.ir

Semnan University

Investigating Tubes Material Selection on Thermal Stress in Shell Side Inlet Zone of a Vertical Shell and Tube Heat Exchanger

Mohammad Mehdi Shoheib [*,a] , Mahdi Hamzehei[b], Shahram Shahrooi[b]

[a] *Young Researchers and Elite Club, Ahvaz branch, Islamic Azad University, Ahvaz, Iran.*
[b] *Department of Mechanical Engineering, College of Engineering, Ahvaz Branch, Islamic Azad University, Ahvaz, Iran.*

PAPER INFO

Paper history:
Received: 2018-03-13
Received: 2018-08-14
Accepted: 2018-08-18

Keywords:
Shell and tube heat exchanger;
Tube material;
Temperature gradient;
Thermal stress.

ABSTRACT

In this study, the effect of the tube material on the thermal stress generated in a vertical shell and tube heat exchanger is investigated. Shell and tube heat exchangers are the most common heat exchangers used in industries. One of the most common failures in these exchangers in the industry is the tube failure at the junction of the tube to tubesheet. When the shell side and the tube side fluid with temperature difference, flow in the heat exchangers, a temperature gradient occurs in the tube. Temperature gradients cause thermal stress in the tube, especially at the junction of the tube to tubesheet where there is no possibility of expansion and contraction. Therefore, in this study, it was tried to make changes in order to reduce the effect of thermal stress in the failure. For this purpose, temperature distribution, thermal stress distribution, and its effects on failure were investigated by changing the material. In order to perform the required analysis, three dimensional models of the inlet zone of the shell side were created, and steady state temperature distribution was obtained, and the stress caused by temperature gradient was analyzed. Because of the interference between fluid and structure in this study, the indirectly coupled field analysis was used. In this way, the thermal analysis results were converted into indirect couple structural analysis as loading. Among the analyzed materials, the lowest rate of stress is for the copper tubes. However, steel tubes have the best safety factor regarding thermal stress.

DOI: 10.22075/jhmtr.2018.13887.1201

1. Introduction

There is a relatively large temperature difference between the shell side and tube side fluids in a shell and tube heat exchanger. For this reason, thermal stress is generally created in the tubes and transmitted to other elements like tubesheet. The temperature difference causes different expansions in the shell and tube that creates thermal stress. If a solution is not considered to deal with it, considerable damage will occur in the exchanger.

Most of the research performed about heat exchanger could be divided into three categories: numerical, experimental, and analytical analysis. In most of the numerical analyses, the effect of physical specifications of exchangers various components have been investigated using available softwares [1-3]. Experimental and analytical analyses have been used to indicate the accuracy of the numerical analysis [4-6].

Ozceyhan and Aluntop [7] studied the temperature distribution, heat transfer, and thermal stress caused by temperature difference in grooved tubes. The study was performed for four different types of grooved tubes and several velocities and temperatures in 2D and steady states. They concluded that maximum thermal stress location in tubes depends on the distance between grooves and volume flow rates. Liu et al. [8] determined the temperature distribution and thermal stress distribution in

[*] *Corresponding Author: M. M. Shoheib, Young Researchers and Elite Club, Ahvaz branch, Islamic Azad University, Ahvaz, Iran.*
Email: m_m_shoheib@iauahvaz.ac.ir.

tubesheet on boilers using the numerical and experimental methods. The result indicated that annular stress was greater than radial stress on the tubesheet. Both of them would be reduced by decreasing the radius and thickness of the tubesheet. Qian et al. [9] studied the residual stress caused by the tube on the tubesheet expansion joint. In this study, experimental and FEM results showed that the residual stress on the interface of tube and tubesheet was not uniform, and there was significantly more stress on the tubesheet surfaces. Li et al. [10] examined the tubesheet crack and failure under several conditions. The results showed that all applied loads were effective on creating the surface cracks and their growing. However, the most effective factor was related to transverse pressure in the exchanger. When crack reached the middle part of the plate thickness, the expansion residual and thermal stresses played the main role in crack growth. Egwanwo and Thaddeus [11] predicted the temperature distribution in a shell and tube heat exchanger using FEM. In their study, three different industrial exchangers were considered, and the field data were compared to the results of the analytical solution. It confirmed the accuracy of the results. Outlet temperature from shell and tubes of the exchanger, heat transfer coefficient and its performance could be predicted with the provided method. Gopichand et al. [12] performed the thermal analysis on a simplified model of shell and tube heat exchanger. They first achieved the thermal analysis using the software and then by governed relations and coding them. Finally, they solved the relations analytically, and by comparing the results of the mentioned methods, they proved the accuracy of the temperature distribution determination in the shell and tube heat exchanger. Ma et al. [13] studied the deformation and thermal stress on internal needle fins in the tubes of shell and tube heat exchangers. The results showed that the maximum temperature gradient in the axial and radial direction would be created when cold fluid flows in the tube and hot fluid flows out of the tube. Heat load was much more effective on deformation and stresses than compressive load. The maximum stress was created on the joins of fin and tube. Xu and Wang [14] studied the residual stresses on weld joint between tube and tubesheet, inlet fluid temperature, and preheating temperature effects. The results showed that maximum residual stress had occurred on the base metal and near the weld surface. Inlet fluid temperature had a little influence on residual stress, and its effect was reduced as the preheating temperature was increased. Zeng et al. [15] examined the lateral fins profile effects on thermal stress in the tubes of a high temperature shell and tube heat exchanger. The results showed that the largest temperature gradient and the maximum thermal stress had occurred on fin joints to tubes. These amounts would be reduced, and the heat transfer rate would be increased by welding fin joints to tube. Parikshit et al. [16] predicted the pressure drop on the shell side of a shell and tube heat exchanger using the concept of the Finite Element Method. In their model, the shell side region was discretized into several elements, and by taking into account the effect of flow pattern, the pressure drop on the shell side was determined. This model took considerably less computation time to predict the pressure drop compared to all other available models. The pressure drop could be predicted up to any point, along the flpa. The model could be applicable to the case of no tubes in the window section. Pal et al. [17] made an attempt to investigate the complex flow and temperature pattern in such a short shell and tube type heat exchanger, with and without baffles in the shell side. In their study, they investigated the effect of flow field on shell side heat transfer coefficient and a comparison with analytical the methods was performed. Wang et al. [18] investigated the thermodynamics performance for the tube banks in cross flow and for the shell sides of shell and tube heat exchangers. Furthermore, the relation between fluid flow and heat transfer was analyzed. The results indicated that the incline degree of tube did not lead to obvious change in characteristics of fluid flow and heat transfer for fl th flowing across the tube banks. Valipour et al. [19] investigated the application of thermal-economic multi-objective optimization of shell and tube heat exchanger using MOBBA. MOBBA method was applied to obtain the maximum effectiveness (heat recovery) and the minimum total cost as two objective functions. Lei et al. [20] investigated two novel shell-and-tube heat exchangers with louver baffles for energy conservation. They utilized the numerical simulations to investigate the thermo-hydraulic performance of the two reformed shell and tube heat exchangers with louver baffles. Fluid flow structures and temperature distributions were used for the analysis of the physical behavior of fluid flow and heat transfer. The temperature distributions in the shell side of the two new shell and tube heat exchangers with louver baffles were more uniform in such a way that it could effectively improve the thermo-hydraulic performance. Mellal et al. [21] studied three-dimensional numerical simulation of turbulent fluid flow and heat transfer in the shell side of a shell and tube heat exchanger. Their study was performed for Reynolds number ranging from 3,000 to 10,000. The numerical results indicated the important role of the studied parameters on the shell side thermal performance enhancement. Abbasian Arani et al. [22] investigated the effect of baffle orientation on shell and tube heat exchanger performance by comparing the pressure drop and heat transfer with a computational fluid dynamic software. They showed that the 90° angle had better performance than other angles of baffle orientation. Ayub et al. [23] tested a unique shell and tube heat exchanger with interstitial twisted tapes with propylene glycol/water solution. The same size conventional shell and tube exchanger with single segmental baffles was also tested under similar temperature and flow conditions. Results from the two exchangers were compared. The new design heat exchanger showed better thermal enhancement index for the whole range of fluid concentrations. Correlations for the Nusselt number and Darcy friction factor were proposed for both heat exchangers.

Providing approaches to reduce the thermal stress in the shell and tube heat exchanger is the purpose of this study. First, the inlet zone of shell side (that is the space between tubesheet and first baffle), including the joint between tube and tubesheet, is modeled and elements are generated. Flow parameters and initial boundary conditions are defined for all boundaries. Thermal analysis is performed, and its results are used as loading for structural analysis. All boundary conditions and necessary parameters are considered in the structural analysis. Then, the analysis is repeated for widely used materials in exchanger construction for determining the effective and appropriate material.

2. Model and Meshes Generation

The analysis was performed in two parts, fluid, and structure. Each model was provided considering the type of analysis, necessary boundary conditions, inputs, and results. First, the shell side inlet zone (the space between tubesheet and the first baffle) of the shell and tube heat exchanger was represented in a 3D model. Then, some reforms, such as creating thickness, were performed on tubes and tubesheet in order to provide them for meshing. This model was used for performing the thermal analysis and obtaining the temperature distribution for tubes. Shell and tube heat exchanger model is shown in Fig. 1. The specifications and physical dimensions are presented in Table 1.

For performing the thermal stress analysis on the tubes, the model was provided separately. The image of the model is shown in Fig. 2. All sizes are the same as previously described.

The O-grid hexagonal elements (3D) were used in meshing so as to produce high quality elements. The method used for meshing and investigating the produced elements quality is completely suggested in the references. Based on the created meshes in this study, the skewness (angular asymmetry) criterion, Eq. (1), is used to investigate the quality of the hexagonal elements.

$$Q_{EAS}(\text{Element equiangle skewness}) = \quad (1)$$

$$1.0 - \max\left\{\frac{\theta_{max} - \theta_e}{180 - \theta_e}, \frac{\theta_e - \theta_{min}}{\theta_e}\right\}$$

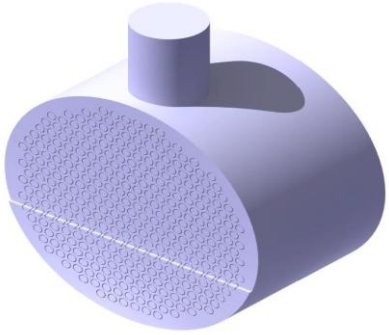

Figure 1. Shell and tube heat exchanger model.

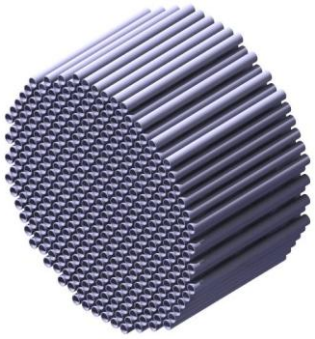

Figure 2. Exchanger tubes model.

Table 1. Physical dimensions.

Components	Size (mm)
Number of tubes	361
Tube outer diameter	19.05
Tube inner diameter	16.56
Nozzle diameter	131
Nozzle height	165
Space between baffle to tubes holder	287
Shell inner diameter	530
Baffle cut height	182.52
Cut baffle percentage	34%
Tube Pitch	23.81
Tubesheet thickness	26

Table 2. Mesh quality distribution (QEAS).

QEAS interval	Amount (%)
$0 \leqslant$ QEAS $\leqslant 0.2$	0.001 %
$0.2 \leqslant$ QEAS $\leqslant 0.4$	0.09 %
$0.4 \leqslant$ QEAS $\leqslant 0.6$	0.74 %
$0.6 \leqslant$ QEAS $\leqslant 1.0$	99.169 %

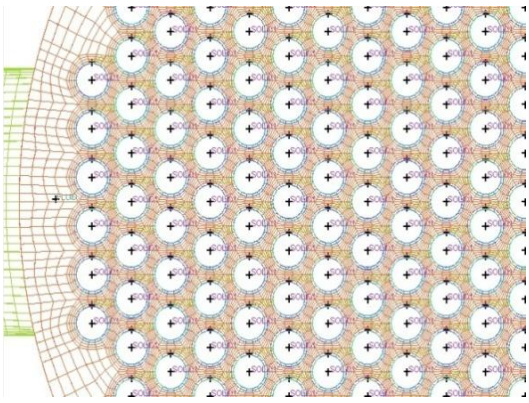

Figure 3. Produced hexagonal blocks around tubes.

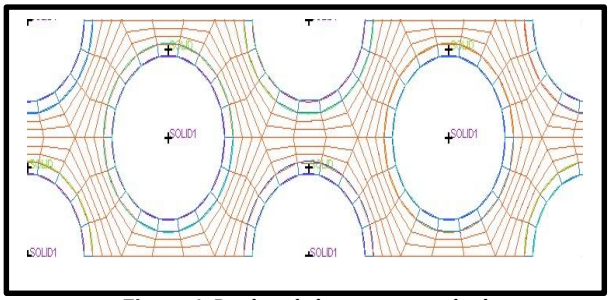

Figure 4. Produced elements around tubes.

where:

θ_{max}: The largest angle between element sides (degree)

θ_{min}: The smallest angle between element sides (degree)

θ_e: The angle of a surface or symmetry element ($\theta_e = 90°$ for hexagonal elements).

In the above equation, QEAS is between 0, and 1 and QEAS=1 indicate the symmetric element. Generally, high quality 2D and 3D meshes include elements with mean values of QEAS between 0.6 and 0.9, respectively [3]. The mesh quality distribution (QEAS) for the model is shown in Table 2.

The illustrations of the mesh are shown in Figs. 3 and 4. As can be seen in Table 2, the produced element quality is more than 99% based on the mentioned criterion.

Meshing model of tubes for structural analysis is similar to the exchanger model for thermal analysis in terms of shape and number of elements. Because of elements location similarity in both models, transferring results was performed with more accuracy and speed when converting from thermal analysis into the structural analysis.

3. Boundary Conditions and Fluids Properties

Data related to the properties of the fluid in the exchanger are provided in Table 3.

Cold fluid (water) is flow in the shell side, and hot fluid (a mixture of gases) is flow in the tube side. Their properties are provided in Table 3. The boundary conditions on tubes were applied as convection between the tube side fluid and the inner surface of the tube, conduction in tube thickness, and convection between the outer surface and the shell side fluid. In order to calculate the heat transfer coefficient of tube side fluid, the experimental method [24] was used; and several effective parameters were considered. Other boundary conditions for thermal analysis are provided in Table 4 [25].

In the second step of the analysis, the boundary conditions on the tubes model, including the support places, forces, and necessary loadings were considered.

4. Turbulence Conditions and Factors

4.1 Turbulence model and solution

After studying the turbulence model types and their applications in different work situations, it was determined that the k-ε (RNG2) model has better performance than others [3]. In this problem, according to the flow type and exchanger performance conditions [12, 14] for discrete algorithms, the simple algorithm was used. First-order upwind and second-order upwind were utilized for solving the momentum and energy equations, respectively.

4.2 Turbulence near the wall

The dimensionless parameter y+ called the dimensionless distance from the wall is used for distinguishing near the wall layers. y+ can be expressed as the ratio between the inertia force and the turbulence force.

Since k-ε turbulence model relations are confirmed only in turbulent flow parts, a new equation should be used near the wall. This relation is called a wall function (wall law).

Table 3. Data on the properties of the fluid in the exchanger.

Property	Unit	Shell side	Tube side
Temperature	oC	30	80
Density	kg/m^3	998.2	2.726
Viscosity	kg/mS	0.001003	137×10-7
Heat capacity	kJ/kg$K$	4.19	0.78
Thermal conductivity	W/mK	0.61	0.013

Table 4. Boundary conditions.

Type of boundary	Boundary conditions
Nozzle inlet	input speed perpendicular to input boundary with 1.9 m/s and 303 K
Baffle window	outflow
The inner wall of tubes	convection with 88.71 W/m2cand 353 K
The outer wall of tubes	coupled
Nozzle wall	insulation
Shell wall	insulation
Baffle wall	insulation
Tube sheet inner wall	coupled
Tube sheet outer wall	insulation
Tube sheet outer surface	insulation
Gravitation acceleration	9.81 m/s^2 in tube direction and opposite to outlet flow from baffle window

[2]Re-normalized group

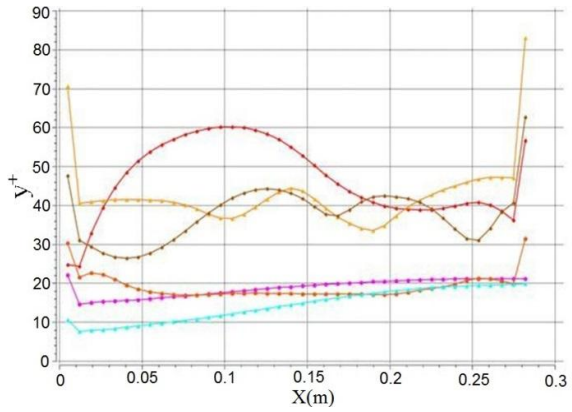

Figure 5. y+ ranges on six walls of the exchanger.

In this analysis, for investigating the accuracy of the k-ε model in turbulent flow parts and wall law relations in areas near the wall, the first node after wall (nearest node to the wall) in the turbulent area was determined. If the node is located out of the turbulent area and under the linear layer, the calculation accuracy would be reduced. In order to solve the problem, meshing should be changed or modified. On the other hand, it should be noted that size and type of mesh are effective on the accuracy of the analysis. According to the reference [3], y+ interval should be in the range of 20-200 for confirming the mentioned conditions. In the analyzed exchanger, 3D model (361 tubes) was used. Investigating y+ for all walls was not possible. So, with an almost uniform distribution, some tubes and exchanger surfaces were selected, and y+ was checked through them. The results from the six selected walls of the exchanger are shown in Fig. 5.

Although y+ of some tubes was out of the range, changing the mesh did not follow the desired results because of other criteria like meshing quality and analysis results accuracy. Therefore, considering all described meshing conditions and criteria, this meshing has the best conditions and results. On the other hand, mean y+ of all exchanger walls is equal to 21.34. Thus, considering Fig. 5 and the mean value of all walls, it can be concluded that y+ range in the most exchanger walls is correct.

5. Results and Discussion

5.1 Independence from element

In order to show the independence of the results of software analysis from conditions and number of model meshing, the sample analysis for aluminum with different conditions and a different number of meshes was performed. According to the studied investigations [3] considering the model conditions, the model with 2203904 elements was considered as the main model. To show the independence of analysis results from the meshing number and conditions, the result (temperature distribution on baffle window) from analysis of the main model was compared with those of a model with more meshes and a model with fewer meshes. Two models with 2712160 and 1632760 meshes were considered as the models with more and fewer meshes, respectively. Finally, the results from their analysis were compared under the same conditions and are presentedin Table 5.

5.2 Thermal and stress analysis

The analysis was done in a steady state, applying available boundary conditions, determining material and its physical properties and other setting and exchanger working conditions. Since the aim of the present study was to investigate the effects of tubes material and tubesheet on thermal stress rate and the tubes material effects on the distribution of temperature [26], the above steps should be performed for various materials.

By investigating the thermal properties of some most applied industrial metals in similar industrial equipment and previous research on heat exchangers, four alloys namely, stainless steel, alloy steel, copper, and aluminum, were selected. These alloys and their physical and mechanical properties are provided in Tables 6 and 8 according to the standards [27]. The analysis was performed for determining the temperature distribution in tubes and tubesheet with considered materials. The result of the thermal analysis on the copper sample is shown in Fig. 6.

Table 5. The comparison of results for different mesh numbers

Number	Original meshes	Modified meshes	Difference
1	2203904	2712160	0.17%
2	2203904	1632760	0.64%

Table 6. Physical properties of different materials

Material	Density (kg/m3)	Specific heat (J/Kg° *K*)	Thermal conductivity (W/m° *K*)
Stainless steel ASTM Al82	8000	500	16.2
Alloy steel ASTM A353	7850	470	52.0
Aluminum ASTM B423	2980	760	180
Copper ASTM B171-C 71500	8940	380	351.34

Table 7. The range of temperature distribution for different materials

Material	Temperature (*K*)	
	minimum	maximum
Stainless steel	303.2	313.1
Alloy steel	303.3	309.6
Aluminum	303.3	306.7
Copper	303.3	306.4

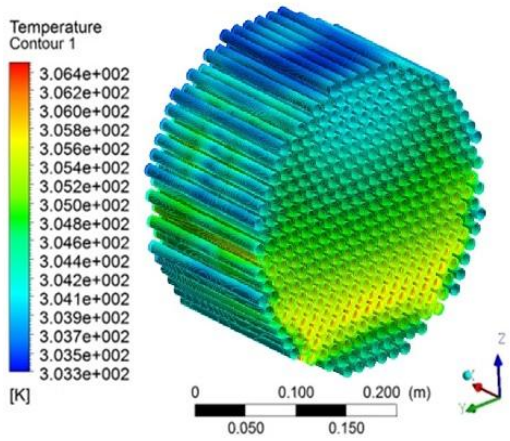

Figure 6. Temperature distributions on copper tubes.

The results of thermal analysis for other samples are the same as the copper sample in terms of temperature distribution state, but the values are different. Temperature range for considered materials is shown in Table 7.

Temperature distribution along the tube (the tube with maximum temperatures) is shown in Fig. 7 for four considered samples. In this Figure, the zero length is from the baffle. With the highest approximation, the temperature distribution in other tubes is also shown. As shown in Fig. 5, the upper tubes located under nozzle have less temperature.

According to the inlet fluid flow lines from the nozzle to the shell (which is shown in Fig. 8), part of it is perverted after dealing with first row tubes, and it flows in the space between shell and tube bundle to the bottom of the exchanger.

Consequently, outer tubes on the tube bundle and their locations on the tubesheet and space between the tube bundle and the shell have less temperature. Temperature distribution in other samples is the same.

As it can be seen in Table 7 and Fig. 7, among the investigated materials, the stainless steel has the highest temperature, and the largest temperature distribution range and copper have the lowest temperature and the smallest temperature distribution range. Furthermore, the most uniform and the most non-uniform distribution are related to copper and stainless steel samples, respectively.

After calculating the temperature distribution in each case, the thermal stress distribution should be determined. The results from thermal stress distribution in the tubes with different material could be compared and discussed. The mechanical properties of considered alloys are provided in Table 8.

The results from stress analysis in the copper sample are shown in Fig. 9. The results from the stress analysis in the tubes of other materials are similar to the copper sample in the stress distribution state, but the values are different. The stress range of the tubes made of different materials is shown in Table 9.

Table 8. Mechanical properties of different materials.

Property / Material	Ultimate tensile	Yield stress	Yang modulus	Poisson factor
	Mpa	Mpa	Gpa	-
Stainless steel	505	215	193	29%
Alloy steel	825	515	200	29%
Aluminum	310	280	255	24%
Copper	340	221	150	32%

Table 9. Maximum and minimum stress in different materials

Material	Minimum(Pa)	Maximum(Pa)
Stainless steel	1.715×107	1.649×107
Alloy steel	1.256×107	7.47×107
Aluminum	3.0×107	1.171×108
Copper	1.406×107	5.488×107

Table 10. Comparing maximum stress values with yield and ultimate stress (Pa).

Material	Maximum stress	Yield stress	Ultimate stress
Stainless steel	1.649×108	215×106	505×106
Alloy steel	7.47×107	505×106	825×106
Aluminum	1.171×108	221×106	340×106
Copper	5.488×107	280×106	310×106

The stress distribution along the tube length with maximum stress on it in four considered samples is shown in Fig. 10. In this Figure, the zero length is from the baffle. Stress distribution in other tubes is in this trend but with different values.

According to the results, the stress analysis of the tubes for the copper sample is shown in Figs. 9 and 10. Considering the temperature distribution among the studied materials, maximum and minimum stress are related to stainless steel and copper, respectively.

As it can be seen in temperature distribution contour, the maximum stress is created in maximum temperature location. The maximum temperature occurs in the tubesheet side edge. Existence of the maximum temperature in this point makes maximum thermal expansion. Because of locating the end of tubes in the tubesheet, which prevents their free expansion, the maximum stress occured in this place. If the maximum stress is more than the yield stress of alloy, it can cause failure on the joint between tube and tubesheet.

In order to determine the best material for manufacturing shell and tube heat exchangers, the stresses created in different materials should be compared with their yield stresses. The maximum stress in the tube and ultimate and yield stress values for considered alloys are provided in Table 10.

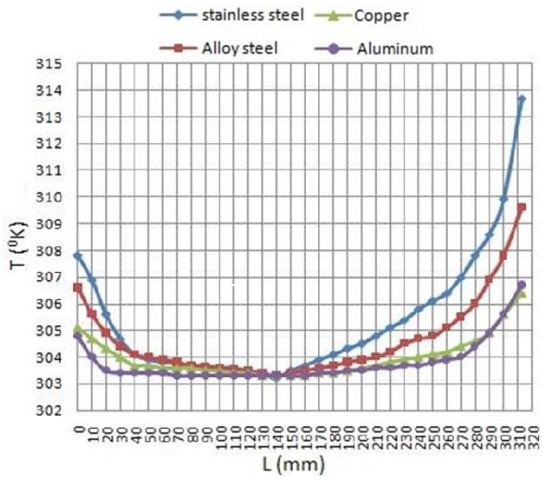

Figure 7. Temperature distributions along the tube with maximum temperature in four samples.

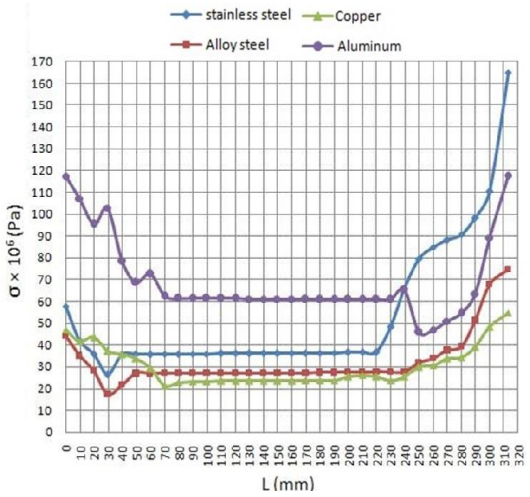

Figure 10. Stress distributions along the tube with maximum stress in four samples.

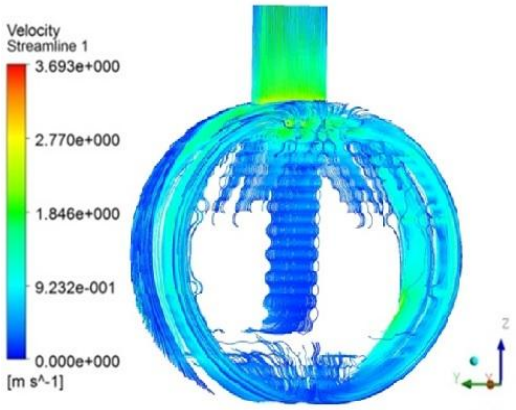

Figure 8. Shell side fluid flow lines.

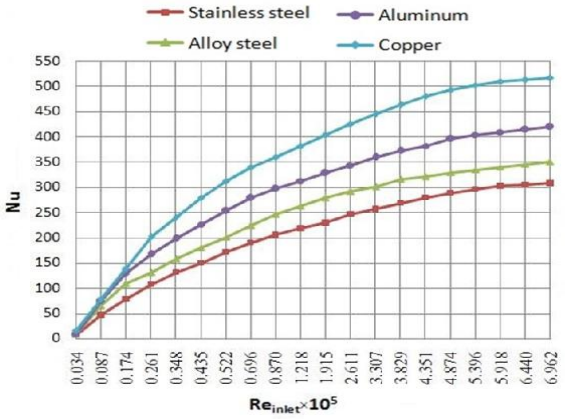

Figure 11. Comparing mean heat transfer for different materials.

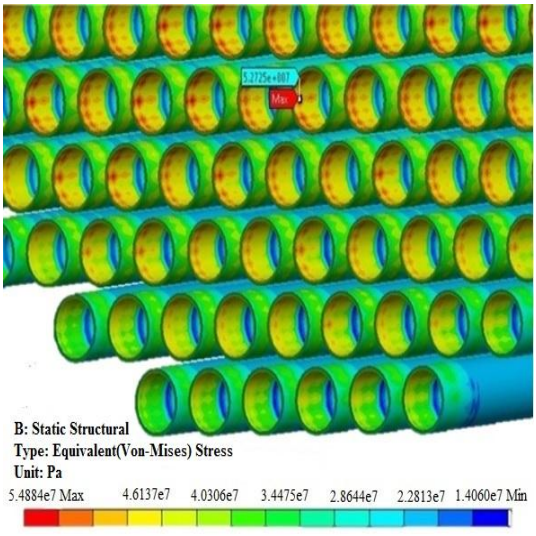

Figure 9. Stress distribution in the copper tubes.

In a stainless steel sample, which has maximum stress, although the maximum stress in tubes is less than the yield stress, the difference between them is not high, and the safety factor is 1.3. Consequently, it is not an appropriate material for heat exchanger in terms of thermal stress.

In an aluminum sample, which is in second-order of thermal stress, the maximum stress is less than the yield stress, and safety factor in tubes is 1.9. As the safety factor is less than the exchanger design safety factor as well as creating stress for other reasons (such as fluid pressure, vibrations, ...), this is lower than results from the reference [28], and for this reason, it is not appropriate.

In alloy steel sample placed in third-order of thermal stress and copper with the lowest thermal stress, the maximum stress created in tube is less than the yield stress. The safety factor for them is equal to 6.76 and 5.1, respectively. As a result, the materials are applicable and appropriate in terms of stress caused in the working conditions.

It is clear that changing the material has a significant effect on temperature and stress distribution in shell and

tube heat exchanger. Therefore, the defects could be prevented by changing the material (in the same working conditions). However, selecting material for exchanger also depends on other conditions like working environment in terms of corrosive and pollutants availability, conditions and chemical properties of cold and hot fluids, heat transfer rate, and so on.

5.3 Heat transfer conditions

Since heat transfer from hot to cold fluid is the purpose of the heat exchanger, applying any changes to it should not reduce the heat transfer irrecoverably. Therefore, the conditions and amount of heat transfer changes should be analyzed in the proposed model. For this reason, the analysis was done in some steps and for different velocities of fluid flow for the investigated alloys. The results were compared under different conditions of turbulence from laminar to turbulent according to Reynolds number value for fluid flow in the tube (calculated with Eq. (2)). The flow is laminar if Reynolds number value is less than 2300; ant it is turbulent if Reynolds number is more than. The results of the heat transfer coefficient in the shell side were expressed in shell side average Nusselt number in terms of Reynolds number. The average Nusselt numbers were reported as one of the results of thermal analysis in each step. It could be reported as shell side Nusselt number (on tube bundle) in the analyzed model. Increasing the average Nusselt number in the shell side indicates the larger values for the heat transfer coefficient. By performing this analysis and investigating mean heat transfer in different samples (which are shown in Fig. 11), it can be seen that copper has the the maximum heat transfer and aluminum, alloy steel, and stainless steel are in next orders.

$$Re = \frac{\rho v d}{\mu} \quad (2)$$

5.4 Validity.

In order to verify the analysis, VDI method was utilized. This method is based on calculating the Nusselt number on tube bundle by experimental relations and comparing it with analysis values. For this purpose, the Nusselt number was obtained using experimental relations on the tube bundle in different velocities of shell side inlet fluid. Then, the same amounts were obtained from analysis in similar conditions of shell side fluid and were compared with the values obtained from the VDI method. In different resources and articles (which used this method for validation of calculations), about 20 percent of error between the the values calculated from equations and the values from analyses are called allowed [29].

In this study, the analysis performed for an aluminum sample was done in 20 different velocities of shell side inlet fluid that created Reynolds number in laminar to fully turbulent range and obtained average Nusselt number in each one. This is the average Nusselt number in the whole exchanger. Moreover, using experimental relations in the same condition, the Nusselt number was calculated on the tube bundle. Obtained results are shown in Fig. 12.

According to Fig. 12, the results of analysis and experimental relations in the low velocity of shell side inlet fluid that caused laminar flow have great difference. With an increase in velocity of inlet fluid and flow turbulence in the shell, this different decreased and in fully turbulent flows, it was in the allowed range. In this study, there is a little difference between the values calculated from two methods for velocity range of shell side inlet fluid; and this difference is in an acceptable range. So, according to this error and the maximum allowed error, the accuracy of the calculations are approved.

5.5 Stress resulting from pressure and temperature difference

When the heat exchanger is operating, it has to withstand not only the temperature load but also the pressure load. The pressure of both sides may have some effects on the stress distribution. In order to investigate the stress distribution condition with the existence of both shell side and tube side fluid pressure and temperature difference, the analysis was performed for the copper sample with simultaneous temperature and pressure distribution.

Comparison between stress distribution of temperature and stress distribution resulting from temperature and pressure along the tube with maximum stress for the copper sample is shown in Fig. 13. The maximum difference between the two stress distributions is 20 percent at its maximum. As it is visible, the stress distribution is more uniform with pressure and temperature, but the place of the maximum stress is the same. Comparison between two distributions and also comparing them with copper yield stress shows that the effect of the pressure distribution of shell side and tube side fluid is much less than temperature.

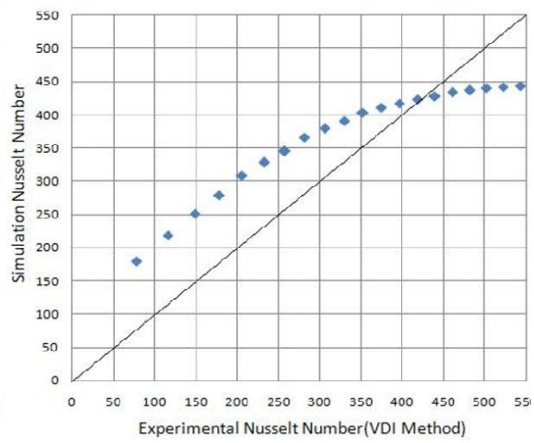

Figure 12. Comparing shell side Nusselt number from FEM and VDI method.

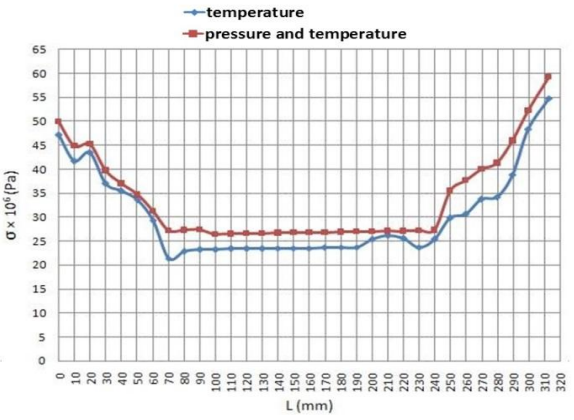

Figure 13. Comparing the stress of temperature with the stress of pressure and temperature in copper.

6. Conclusions

Among the considered materials, stainless steel has the highest temperature and the largest temperature distribution range; while copper has the lowest temperature and the smallest range. Also, the most uniform and non-uniform temperature distribution are related to copper and stainless steel, respectively. Because of the existence of hot fluid in the tube and arrival of cold fluid from the nozzle to shell, the highest temperature in all models occurred at the end of the opposite side of the nozzle. The maximum stress is related to stainless steel, and the lowest amount is related to the copper sample. Alloy steel is the best material for constructing the heat exchanger in terms of maximum thermal stress. It has the most safety factor among the samples. Copper is the next one in terms of maximum thermal stress. Aluminum and stainless steel samples are not appropriate from this point of view. Copper has the most heat transfer, and aluminum, alloy steel, and stainless steel are in the next orders. According to the temperature, stress distribution, and heat transfer rate in different samples, it can be concluded that copper has the best condition.

Nomenclature

$k-\varepsilon$	Turbulence model
L	Length(mm)
Nu	Nusslet number(dimensionless)
Q_{EAS}	Element equiangle skewness
θ_{max}	The largest angle between element sides (degree)
θ_{min}	The smallest angle between element sides (degree)
θ_e	The angle of a surface or symmetry element (degree)
Re	Reynolds number(dimensionless)
T	Temperature
X	Length(m)
y+	Dimensionless distance from the wall
ρ	Fluid density
v	Fluid speed
μ	Viscosity

References

[1] M. S. Liu, Dong, Q. W. Dong, Wang, D.-B. Wang, X. Ling, Numerical simulation of thermal stress in tube-sheet of heat transfer equipment, International journal of pressure vessels and piping, 76(10), 671-675, (1999).

[2] M. K. Apalak, R. Güneş, L. Fídanci, Geometrically non-linear thermal stress analysis of an adhesively bonded tubular single lap joint, Finite elements in analysis and design, 39(3), 155-174, (2003).

[3] K. Mohammadi, Investigation of the effects of baffle orientation, baffle cut and fluid viscosity on shell side pressure drop and heat transfer coefficient in an e-type shell and tube heat exchanger, PhD thesis, University of Stuttgart: Stuttgart. (2011).

[4] H. Cho, G. Kardomateas, Thermal shock stresses due to heat convection at a bounding surface in a thick orthotropic cylindrical shell, International journal of solids and structures, 38(16), 2769-2788, (2001).

[5] W. Jin, Z. Gao, L. Liang, J. Zheng, K. Zhang, Comparison of two FEA models for calculating stresses in shell-and-tube heat exchanger, International journal of pressure vessels and piping, 81(6), 563-567, (2004).

[6] G. Xie, Q. Wang, M. Zeng, L. Luo, Heat transfer analysis for shell-and-tube heat exchangers with experimental data by artificial neural networks approach, Applied Thermal Engineering, 27(5), 1096-1104, (2007).

[7] V. Özceyhan, N. Altuntop, Heat transfer and thermal stress analysis in grooved tubes, Sadhana, 30(4), 537-553, (2005).

[8] M. Liu, Q. Dong, X. Gu, Stress analysis of Ω-tubesheet in waste heat boiler, Journal of Pressure Equipment and Systems, 4, 1-12, (2006).

[9] C. Qian, C. Duan, H. Yu, H. Duan, J. Tian, Reliability study of the hydraulically expanded tube-to-tubesheet joint, Journal of pressure vessel technology, 128(3), 408-413, (2006).

[10] H. Li, C. Qian, Q. Yuan, Cracking simulation of a tubesheet under different loadings, Theoretical and Applied Fracture Mechanics, 54(1), 27-36, (2010).

[11] V. Egwanwo, B. T. Lebele-Alawa, Prediction of the temperature distribution in a shell and tube heat exchanger using finite element model, Canadian Journal on Mechanical Science and Engineering, 3, 72-82, (2012).

[12] A. GopiChand, A. Sharma, G.V. Kumar, A. Srividya, Thermal analysis of shell and tube heat exchanger using mat lab and floefd software. International Journal of Reasearch In Engineering And Technology, 1(3), 276 - 281, (2012).

[13] T. Ma, Y. Chen, M. Zeng, Q. Wang, Stress analysis of internally finned bayonet tube in a high temperature heat exchanger, Applied Thermal Engineering, 43, 101-108, (2012).

[14] S. Xu, W. Wang, Numerical investigation on weld residual stresses in tube to tube sheet joint of a heat exchanger, International Journal of Pressure Vessels and Piping, 101, 37-44, (2013).

[15] M. Zeng, T. Ma, B. Sundén, M. B. Trabia, Q. Wang, Effect of lateral fin profiles on stress performance of internally finned tubes in a high temperature heat exchanger, Applied Thermal Engineering, 50(1), 886-895, (2013).

[16] B. Parikshit, K. Spandana, V. Krishna, T. Seetharam, K. Seetharamu, A simple method to calculate shell side fluid pressure drop in a shell and tube heat exchanger, International Journal of Heat and Mass Transfer, 84, 700-712, (2015).

[17] E. Pal, I. Kumar, J. B. Joshi, N. Maheshwari, CFD simulations of shell-side flow in a shell-and-tube type heat exchanger with and without baffles, Chemical Engineering Science, 143, 314-340, (2016).

[18] Y. Wang, X. Gu, Z. Jin, K. Wang, Characteristics of heat transfer for tube banks in crossflow and its relation with that in shell-and-tube heat exchangers, International Journal of Heat and Mass Transfer, 93, 584-594, (2016).

[19] M. S. Valipour, M. Biglari, E. Assareh, Thermal-economic optimization of shell and tube heat exchanger using a new multi-objective optimization method. Journal of Heat and Mass Transfer Research, 1, 67-78, (2016).

[20] Y. Lei, Y. Li, S. Jing, C. Song, Y. Lyu, F. Wang, Design and performance analysis of the novel shell-and-tube heat exchangers with louver baffles, Applied Thermal Engineering, 125, 870-879, (2017).

[21] M. Mellal, R. Benzeguir, D. Sahel, H. Ameur, Hydro-thermal shell-side performance evaluation of a shell and tube heat exchanger under different baffle arrangement and orientation, International Journal of Thermal Sciences, 121, 138-149, (2017).

[22] H. Uosofvand, A. A. Abbasian Arani, A. Arefmanesh, Effect of baffle orientation on shell-and-tube heat exchanger performance, Journal of Heat and Mass Transfer Research, 4, 83-90, (2017).

[23] Z. H. Ayub, D. Yang, T. S. Khan, E. Al-Hajri, A.H. Ayub, Performance characteristics of a novel shell and tube heat exchanger with shell side interstitial twisted tapes for viscous fluids application, Applied Thermal Engineering, 134, 248-255, (2018).

[24] E. Cao, Heat transfer in process engineering, McGraw Hill Professional, (2009).

[25] A. Aziz, M. Torabi, Thermal stresses in a hollow cylinder with convective boundary conditions on the inside and outside Surfaces, Journal of Thermal Stresses, 36(10), 1096-1111, (2013).

[26] J. H. Zhang, G. Z. Li, S. R. Li, Y. B. Ma, DQM-Based Thermal Stresses Analysis of a Functionally Graded Cylindrical Shell Under Thermal Shock, Journal of Thermal Stresses, 38(9), 959-982, (2015).

[27] P. D. Harvey, Engineering properties of steel, American Society for Metals Metals Park, Ohio, (1982).

[28] A. P. Fraas, Heat exchanger design, John Wiley & Sons, (1989).

[29] V. Gesellschaft, V. G. Chemieingenieurwesen, VDI Heat Atlas, Springer Science & Business Media, (2010).